Available online at www.sciencedirect.com
SCIENCE DIRECT®

Polymer 46 (2005) 8113–8118

polymer

www.elsevier.com/locate/polymer

Ionic conductivity studies of poly(ethylene oxide)–lithium salt electrolytes in high-pressure carbon dioxide

Yoichi Tominaga, Shingo Hirahara, Shigeo Asai, Masao Sumita*

Department of Chemistry and Materials Science, Tokyo Institute of Technology, Ookayama, Tokyo 152-8552, Japan

Received 7 February 2005; received in revised form 5 May 2005; accepted 22 May 2005
Available online 15 June 2005

Abstract

We have measured ionic conductivity of PEO–LiX [anion X = $N(CF_3SO_2)_2$ (TFSI), ClO_4, CF_3SO_3, BF_4, NO_3, and CH_3SO_3] polymer electrolytes in CO_2 at pressures varied from 0.1 to 20 MPa. From the temperature dependence in supercritical CO_2, a large increase in the conductivity for PEO–$LiBF_4$ and $LiCF_3SO_3$ electrolytes has been observed. Permeation of the CO_2 molecules gave rise to the plasticization for crystal domains in the electrolytes, which is related to the reduction in transition point of the Arrhenius plot corresponding to the melting of crystal PEO. Relation between the conductivity and CO_2 reduced density revealed that the electrolytes containing fluorinated anions such as 'CO_2-philic' BF_4 and CF_3SO_3 increase in the conductivity with increasing the density. This indicates that the salt dissociation was promoted by the CO_2 permeation and the Lewis acid–base interactions between fluorinated anions and CO_2 molecules.

Keywords: Poly(ethylene oxide); Carbon dioxide; Ionic conductivity

1. Introduction

Ion-conductive polymer electrolytes have been increasingly proposing as solid-state alternatives to liquid electrolytes in electrochemical device applications such as polymer batteries [1–4], since ionic conduction in poly(ethylene oxide) (PEO)-alkali metal salt mixtures was first reported by Wright [5]. However, these materials suffer from a lower conductivity in the solid-state than most liquid, gel, and ceramic electrolytes. Since, ions are transported via the segmental motion of ether chains, fast migration of ions in polymer can be realized by increasing the local chain mobility. The localized structure that is central to ionic conduction is believed to involve cation–anion or cation–dipole interactions [6]. Unfortunately, the ionic interaction sometimes inhibits migration of ions because of their strong cohesion, which increases the glass transition temperature T_g. For fast migration of ions, a technique is needed to modify the localized polar structure containing ions.

Recently, we have reported that processing into high-pressure CO_2, especially in the supercritical CO_2 ($scCO_2$), is effective in improving the conductivity of polymer electrolytes in the solid state, since there is a large increase in the room temperature conductivity of PEO [7,8] and poly[oligo(oxyethylene glycol)methacrylate] (PMEO) [9, 10] containing $LiCF_3SO_3$ with CO_2 as a processing solvent. In these works, two effects of $scCO_2$ processing were expected; one is plasticization of amorphous domains, where ionic conduction occurs, and the other is dissociation of ionic species such as the aggregator and crystalline complex, which is largely responsible for increase in T_g. Certainly the CO_2 is known to be a good solvent for polymer synthesis and processing [11,12]. During the polymer processing, the solubility of CO_2 in many polymers is substantial and can lead to a dramatic decrease in T_g, namely plasticization [13,14]. On the other hand, it has been reported that the CO_2 molecules can permeate into polymers, especially in the amorphous region, and have specific interactions with some polymers, which possess electron-donating groups such as carbonyl groups [15]. In our previous work, it is considered that the CO_2 molecules act as a promoter for the dissociation of aggregated ions in PEO, improving the conductivity according to the Lewis acid–base interactions [8]. For understanding above

---

* Corresponding author. Tel.: +81 3 5734 2431; fax: +81 3 5734 2876.
E-mail address: msumita@o.cc.titech.ac.jp (M. Sumita).

0032-3861/$ - see front matter © 2005 Elsevier Ltd. All rights reserved.
doi:10.1016/j.polymer.2005.05.091

behavior, it is necessary to measure direct influence on the ion transport properties in high-pressure CO_2.

We have already measured the conductivity in PEO- and PMEO-$LiCF_3SO_3$ electrolytes in CO_2 [16]. A large increase in the conductivity under the high-pressure conditions has been demonstrated for both PEO and PMEO electrolytes. However, it is known that the conductivity of simple polyether electrolytes usually decreases with increasing pressure in high-pressure inert gas such as N_2 or Ar [17–21]. Therefore, measurements in CO_2 are of interest as an 'activated solvent' system for polyether electrolytes compared with the inert gases. In this paper, the isobaric conductivity of PEO electrolytes containing lithium salts, $LiN(SO_2CF_3)_2$, $LiCF_3SO_3$, $LiClO_4$, $LiBF_4$, $LiNO_3$, and $LiCH_3SO_3$, have been measured in CO_2. Influence of the salt species on the conductivity in CO_2 has been evaluated as a function of CO_2 reduced densities.

2. Experimental section

An electrolyte film was prepared from PEO ($M_w = 5 \times 10^5$, Wako Chemical Co.) and lithium salt. The salts used in this study are LiX [anion X; TFSI (bis-(trifluoromethane sulfonyl)imide, 3M Co.), BF_4 (ACROS Organics Co.), NO_3, ClO_4 (Kanto Chemical Co.), CF_3SO_3 (Aldrich Co.), and CH_3SO_3]. The salt, $LiCH_3SO_3$, was prepared from neutralization of LiOH (0.1 mol, Fluka Co.) and CH_3SO_3H (0.12 mol, Kanto Chemical Co.) in distilled water, following it was washed by excess acetone for three times and dried in vacuo at 100 °C for 24 h (yield: 76.8%). The PEO and salt were dissolved in excess acetone (special grade, Kanto Chemical Co.) and mixed at 60 °C for 24 h. The ratio of Li ion concentration to oxyethylene (OE) unit in PEO was arranged to be 10 mol% ($[Li^+]/[OE] = 1/10$). The intermediate gel-like solution was then slowly dried at 60 °C. The resulting solid product ($PEO_{10}LiX$) was compression-molded for 10 min into a film approximately 1.0 mm-thick at 80 °C under a pressure of 19.6 MPa, and then dried in vacuo at room temperature for 24 h.

The DSC measurement for $PEO_{10}LiX$ was carried out using a Shimadzu Co. system consisting of a DSC-50 and TA-50WS under dry N_2. The temperature was increased from −100 to 200 °C at a heating rate of 10 °C/min.

The experimental apparatus for impedance measurement used in this study is the same as that in our previous report [16]. The supercritical CO_2 extraction system (JASCO Co.) consists of a delivery pump (SCF-Get), an automatic backpressure regulator (SCF-Bpg), and a heater. A high-pressure original reactor (max. 30 MPa, 200 °C) was constructed from a retainer and a vessel (50 ml) with a poly(ether ether ketone) (PEEK) seal. Carbon dioxide was pumped into the reactor from a gas cylinder (99.95%, Showa Tansan Co). The reactor has six access ports on the surface of the retainer, and threaded fixtures on the flat surfaces. A sheathed thermocouple (1.6 mm-diameter) made from Inconel was introduced into the reactor. SUS tubes were used for the inflow and outflow of liquid CO_2. Pt wire (0.4 mm-diameter) insulated by a PEEK tube was fixed on the side of a SUS plate (15×15 mm^2, 0.5 mm-thick) for use as electrodes. A Teflon® plate (1.0 mm-thick) was used as a spacer between two SUS electrodes. The sample was sandwiched between the SUS electrodes with a spacer, and the cell surface was insulated by polyimide tape. The cell was dried at 100 °C for 12 h, and was cooled down to room temperature in vacuo for at least 24 h before measurement. The ionic conductivity was measured by the complex impedance method using a Solartron 1260 Impedance Analyzer (Schlumberger) in the frequency range 100–20 MHz. The cell was loaded in the reactor, which was filled with neat CO_2 and vented to atmospheric pressure three times. The CO_2 pressure was then increased up to each measurement pressure, and maintained with a flow rate of 1 ml/min. After the pressure stabilized, the reactor was heated slowly from room temperature to 100 °C. The temperature was held constant, every 10 °C interval for at least 20 min, following which the impedance measurement was carried out. The conductivity under N_2 was also measured using the same system in a SUS box filled with dry N_2. The temperature was increased from 30 to 100 °C at a heating rate of 2.0 °C/min using a temperature controller (KP-1000, CHINO Co).

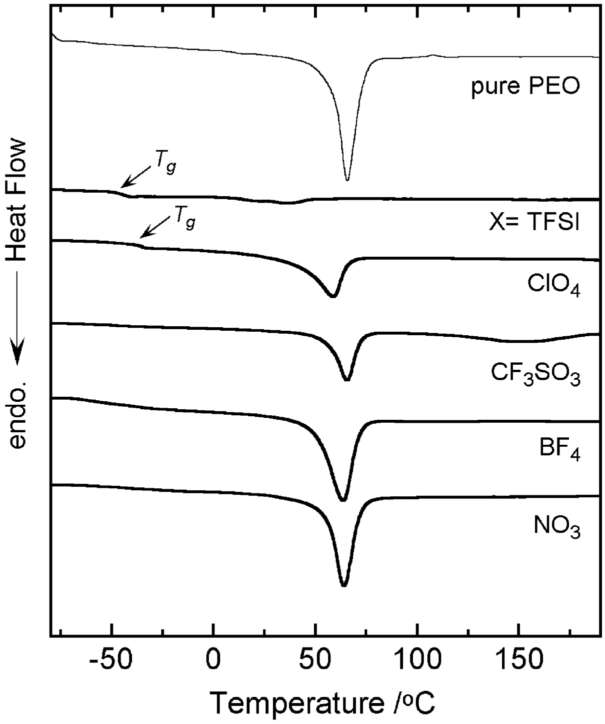

Fig. 1. DSC curves of neat PEO and $PEO_{10}LiX$ electrolytes.

3. Results and discussion

Fig. 1 shows various DSC curves of neat PEO and $PEO_{10}LiX$ electrolytes. The DSC data of all samples are summarized in Table 1. A strong endothermic peak at 67 °C corresponding to the melting of crystal PEO T_m, was clearly observed in neat PEO. There is no glass transition in the neat PEO because of its high crystallinity. On the other hand, the T_m and heat of fusion ΔH, which is in proportion to crystallinity, decreases as the Li salts are added to the PEO as a result of the change of local structure caused by the ion–dipole interactions between the Li cation and the oxygens of ether chains in amorphous regions which inhibits the crystallization. In particular, PEO–LiTFSI electrolyte is almost amorphous state with a glass transition temperature T_g, at −49 °C. The LiTFSI is well known as highly soluble salt, which has been widely applied for electrolytes, because the anion charge is delocalized by the strong electron-withdrawing effect of trifluoromethyl groups [22]. Moreover, the dissolved anion acts as a plasticizer in PEO [22]. A weak endothermic peak, which is attributed to the disordered nature of the crystal PEO domains, was confirmed in PEO–$LiClO_4$ and $LiCF_3SO_3$ electrolytes. The PEO–$LiCF_3SO_3$ possesses another broad endothermic peak at 152 °C ($\Delta H = 51$ J/g) corresponding to the presence of crystalline complex domains [23]. From the Table 1, it seems that the T_m and ΔH decreases with increasing dissociation degree of Li salts, namely, decreasing the lattice energy.

Fig. 2 shows elapsed time dependence of ionic conductivity for $PEO_{10}LiCF_3SO_3$ at 90 °C in supercritical CO_2. This figure reveals that the conductivity at both 10 and 20 MPa gradually increase with increasing the time, and then reach to constant value at approximately 60 min. This means that the CO_2 molecules gradually permeated into the sample and were saturated. It has been reported that the permeation and swelling give rise to the relaxation of polymer chains mainly in the amorphous region, which is related to the decrease in T_g and in the amount of crystalline domains [13,14]. In addition, the sample at 20 MPa exhibits slightly higher conductivity. This is probably due to the difference in density of CO_2 that was pressurized at 10 and 20 MPa.

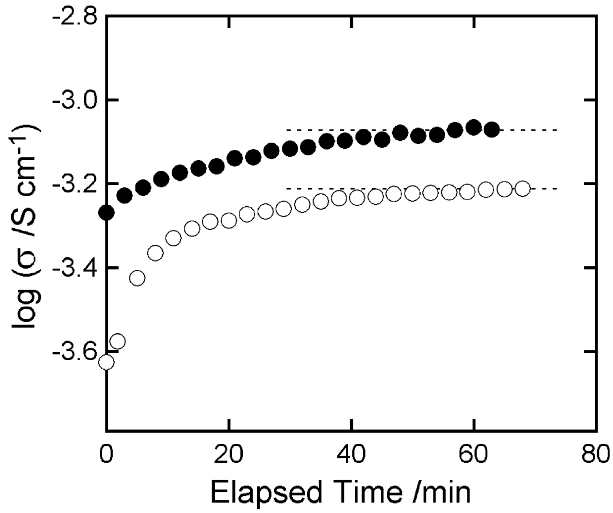

Fig. 2. Elapsed time dependence of ionic conductivity for $PEO_{10}LiCF_3SO_3$ at 90 °C in CO_2 pressurized at (○) 10 MPa and (●) 20 MPa.

Temperature dependences of ionic conductivity for all $PEO_{10}LiX$ electrolytes in N_2 and CO_2 are shown in Figs. 3–5. In the N_2 condition, the ion-conductive behavior of these PEO-based electrolytes can clearly be compared. Transition points of PEO–$LiBF_4$, $LiCF_3SO_3$, $LiNO_3$, and $LiCH_3SO_3$ electrolytes at approximately 60 °C are due to the melting of crystal PEO corresponding to the strong endothermic peak as seen in Fig. 1. The $LiCH_3SO_3$ electrolyte shows the lowest conductivities in all samples because of the low solubility of added salt. On the other hand, the LiTFSI electrolyte shows quite high conductivities and has no transition at entire measurement temperature. This indicates that the solubility of LiTFSI is certainly high and the anion may possess a plasticizing effect on PEO. Fig. 4 shows the temperature dependence of the conductivity in CO_2 at 0.1 MPa. In the experiment of Fig. 4, CO_2 is completely gas

Table 1
Glass transition temperature (T_g), melting point (T_m, peak top), and heat of fusion (ΔH) for $PEO_{10}LiX$ electrolytes from DSC measurement

Sample	T_g (°C)	T_m (°C)	ΔH (J/g)
Neat PEO	–	67	153
X = TFSI	−49	36	22
ClO_4	−38	59	80
CF_3SO_3	–	66	81
BF_4	–	64	130
NO_3	–	64	138

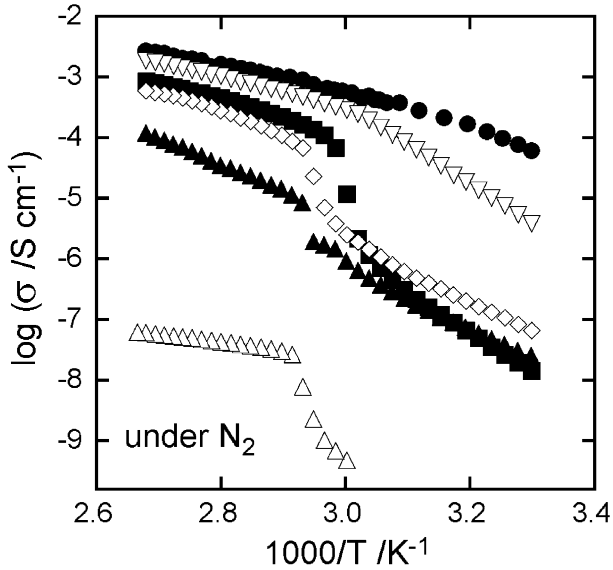

Fig. 3. Temperature dependence of ionic conductivity for $PEO_{10}LiX$ electrolytes [X; (●) TFSI, (▽) ClO_4, (▲) CF_3SO_3, (■) BF_4, (◇) NO_3, and (△) CH_3SO_3] in N_2.

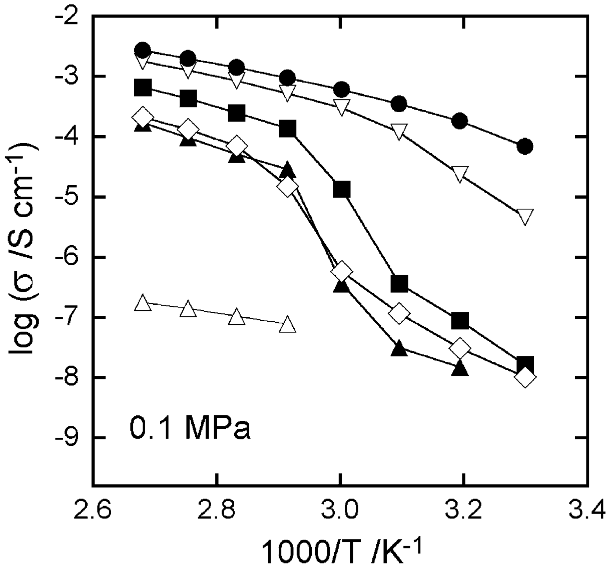

Fig. 4. Temperature dependence of ionic conductivity for $PEO_{10}LiX$ electrolytes in CO_2 at 0.1 MPa. Symbols are the same as those in Fig. 3.

state at 0.1 MPa and at the measurement temperature between 30 and 100 °C. Variations in the conductivity are quite similar to that in the inert N_2 gas as seen in Fig. 3. Therefore, we can say that there is no plasticizing effect of CO_2 on the samples at the atmospheric pressure. The PEO–LiTFSI and $LiClO_4$ electrolytes exhibit relatively high conductivity without large decrease in the conductivity at low temperature corresponding to the melting of crystal PEO. The Arrhenius plot of the LiTFSI electrolyte is convex throughout the entire temperature range, and exhibits similar behavior to other amorphous-type polyether electrolytes. On the other hand, the conductivity of other electrolytes is low at room temperature as compared with the PEO–LiTFSI. The PEO–$LiCF_3SO_3$ electrolyte shows low conductivity at room temperature because of the presence of crystalline complex domains. The data below 60 °C for $LiCH_3SO_3$ electrolyte was impossible to measure because of its extremely low conductivity. Fig. 5 also shows the temperature dependence of the conductivity in CO_2 at 20 MPa. The conduction behavior at 20 MPa is clearly different with the data in Fig. 4. In this condition, CO_2 can easily permeate into the samples because it is near-critical or supercritical fluid with highly densities as compared with the gas state. The transition points of PEO–$LiBF_4$, $LiCF_3SO_3$, $LiNO_3$, and $LiCH_3SO_3$ electrolytes corresponding to the melting of crystal PEO shift apparently to lower temperatures. The slope of the Arrhenius plots, showing the apparent activation energy, is also lowered by the pressurization. These indicate that the permeation of CO_2 molecules gave rise to the plasticization for crystalline PEO domains. The conductivity of PEO–$LiBF_4$ and $LiCF_3SO_3$ electrolytes markedly increases at entire measurement temperature, whereas the electrolytes generally exhibits negative pressure dependence of the conductivity in inert gas such as N_2 or Ar [17–21]. This means that CO_2 molecules that permeated into the PEO electrolytes are quite effective for enhancement in the conductivity. However, it seems that there is almost no difference in the conductivity of PEO–LiTFSI, $LiClO_4$, and $LiNO_3$ electrolytes between at 0.1 and at 20 MPa. It is considered that there may be some dependence of anion or salt species on the conductivity in high-pressure CO_2.

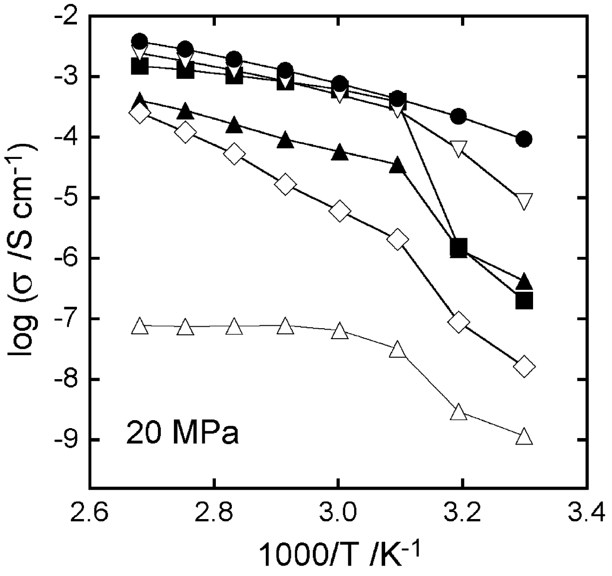

Fig. 5. Temperature dependence of ionic conductivity for $PEO_{10}LiX$ electrolytes in CO_2 at 20 MPa. Symbols are the same as those in Fig. 3.

Supercritical CO_2 is highly compressible and the density can be tuned over a wide range by varying pressure. The tunable property gives rise to the solvation for small molecules (or swelling for polymers), namely solute–solvent clustering [12], which is defined as a local solvent density. This means that CO_2 acts as ‘active solvent’ and the property may be exploited in the plasticization of polymers or in the dissociation of salts by pressure control. Here, we

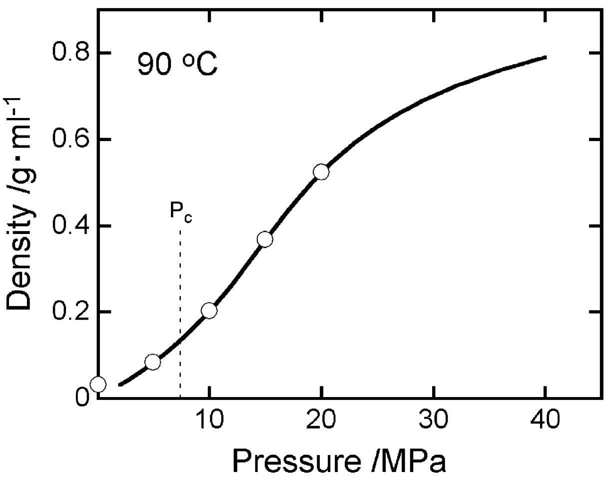

Fig. 6. Variation in density (ρ) of pure CO_2 at 90 °C. The symbol (○) emphatically indicates the data that were used in Figs. 7 and 8.

show typical variation in density of pure CO_2 (ρ) at 90 °C in Fig. 6. Pressure dependence of the density as a line has been calculated by Lee and Kesler method which developed a modified Benedict–Webb–Rubin (BWR) equation within the context of Pitzer's three-parameter correlation [24]. Below the critical pressure P_c, CO_2 density as the gas state is very low, to be less than 0.1 g/cm^3. At the near-critical or supercritical region, the density increases exponentially with increasing the pressure, and is more than 0.5 g/cm^3 at 20 MPa. Fig. 7 shows variation in the conductivities of $PEO_{10}LiX$ electrolytes at 90 °C as a function of CO_2 reduced densities ($\rho_r = \rho/\rho_c$, where ρ_c is the critical density, 0.468 g/ml [25]). This figure reveals that the ionic conduction in PEO is strongly affected by the change of CO_2 density. Moreover, difference in the conduction behavior between these electrolytes based on the anion species was clearly confirmed. In the near-critical or supercritical region, the PEO–$LiCF_3SO_3$ and $LiBF_4$ electrolytes exhibit sinusoidal increase in the conductivity with increasing the density, whereas the conductivity of PEO–LiTFSI and $LiClO_4$ electrolytes is practically invariable. However, PEO–$LiNO_3$ electrolyte only exhibits negative dependence of the conductivity in the high-density region. These results indicate that the salt species influence on ion-conductive behavior of the electrolytes in CO_2, i.e. the anion which possesses highly electronegative atoms such as fluorine may be related to the enhancement in CO_2 solubility. Probably, dissociated anions such as BF_4 and CF_3SO_3 easily form solute–solvent clusters with CO_2 molecules which permeated into the sample. The conductivity of PEO–LiTFSI electrolyte is almost the constant at high pressures, in spite that the salt possesses six fluorine atoms in anion. Effect of CO_2 on the conductivity is small at the high-density region, because the salt is basically high dissociable salt in PEO. In addition, rapid increases in the conductivity in the low-density region between 0 and 0.4 have been observed for all electrolytes. This characteristic pattern is a reflection of the specific solute–solvent interactions occurring in the two density regions; one is the low-density region 0–0.5 and the other is the near-critical or supercritical region 0.5–1.5 showing a plateau-like response [12]. In Fig. 7, only $LiNO_3$ electrolyte shows negative dependence of the conductivity in the subcritical and supercritical regions, whereas it has positive dependence in the low-density regions. This is probably due to the CO_2-phobic nature of added $LiNO_3$.

Numerous experimental investigations, which focus on the interactions between CO_2 and organic molecules or polymers under high-pressures, have been reported [15,26–28]. For example, Abbott et al. have studied on the electrochemical properties of ammonium-type electrolytes in CO_2 and concluded that the solubility is further increased by halogenation of the organic group [26]. Fedkiw et al. have reported that ionic conductivity of alkali metal trifluoroacetate salts in CO_2 is much higher than that of the acetates [27]. They discuss on the results that the interaction between the quadrupole moment of CO_2 and the dipoles of CF_3 group makes the salt more CO_2-philic [28], leading to an increase in the solubility. Therefore, we prepared $LiCH_3SO_3$ as a simple salt model to compare with the $LiCF_3SO_3$ system. Fig. 8 compares the conductivity of $PEO_{10}LiCH_3SO_3$ and $LiCF_3SO_3$ electrolytes at 90 °C as a function of CO_2 reduced densities. This reveals that the conductivity of PEO–$LiCH_3SO_3$ electrolyte sinusoidal decreases with increasing the density as same as the $LiNO_3$ system in Fig. 7. Generally, the salts, $LiCH_3SO_3$ and $LiNO_3$, possess relatively high lattice energy; therefore, it is basically hard to dissolve into high molecular weight polyethers and to exhibit relatively good conductivity. These salts are considered to form mainly aggregate ions in

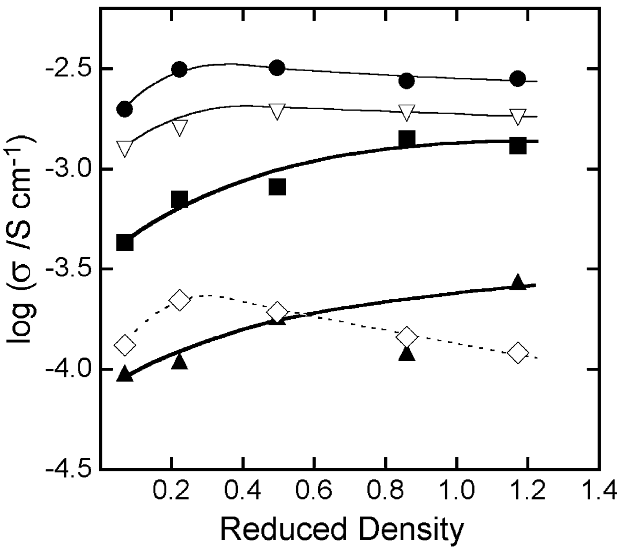

Fig. 7. Ionic conductivities of $PEO_{10}LiX$ electrolytes at 90 °C as a function of CO_2 reduced densities. Symbols are the same as those in Fig. 3.

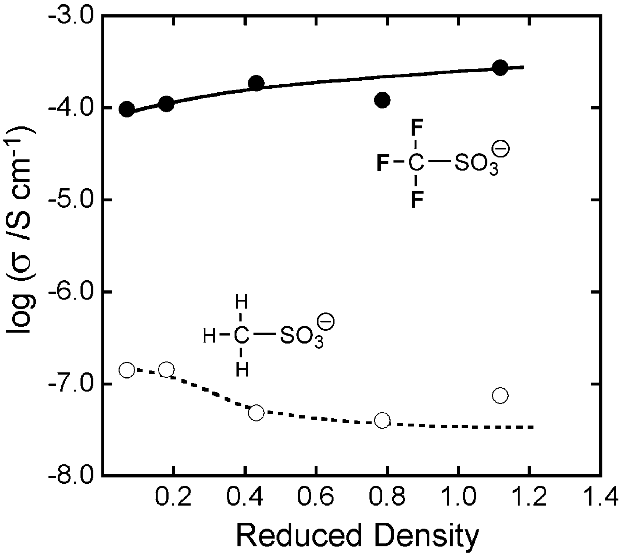

Fig. 8. Ionic conductivities of (●) $PEO_{10}LiCF_3SO_3$ and (○) PEO_{10}-$LiCH_3SO_3$ electrolytes at 90 °C as a function of CO_2 reduced densities.

polyethers, which are related to the inhibition of local segmental motion and give rise to the increase in T_g. On the other hand, the conductivity of PEO–$LiCF_3SO_3$ electrolyte increases with increasing the density, whereas it contains highly crystalline complex domains, which inhibit the migration of carrier ions. In the $LiCF_3SO_3$ system, dissociation of aggregate anions or the complex domains to smaller ions may be caused through the permeation of CO_2. We believe that this is based on the Lewis acid–base interactions between CO_2 molecules and fluorine atoms (or CF_3 groups), leading to the CO_2-philic nature. The existence of CO_2–anion interactions in PEO gives rise to the increase in carrier ions, following enhancement in the conductivity.

4. Conclusions

Ionic conductivity of PEO-based polymer electrolytes containing LiX (X = TFSI, ClO_4, CF_3SO_3, BF_4, NO_3, and CH_3SO_3) has been measured in CO_2 at pressures up to 20 MPa. Apparent difference in the conductivity for $PEO_{10}LiX$ electrolytes between at atmospheric and at high pressures was found. Temperature dependence of the conductivity in CO_2 at the atmospheric pressure showed quite similar behavior to that in N_2 gas. The Arrhenius plots at 20 MPa revealed a large increase in the conductivity for PEO–$LiBF_4$ and $LiCF_3SO_3$ electrolytes and a reduction in the transition point corresponding to the melting of crystal PEO. Permeation of CO_2 molecules into PEO gave rise to the plasticization for the crystal domains. Relation between the conductivity and CO_2 reduced density indicated that the electrolytes containing fluorinated anions such as BF_4 and CF_3SO_3 increase in the conductivity with increasing the density. Probably, dissociation of the salt was promoted by the permeation of CO_2 molecules. This indicates that these anions are basically CO_2-philic. In the pressurized CO_2 conditions, the anions may interact preferentially with the CO_2 molecules rather than the oxyethylene chains, which are based on the Lewis acid–base nature.

Acknowledgements

One of the authors (Y.T.) acknowledges the financial support for young scientist from the Ministry of Education, Science, Sport, and Technology, Japan (No. 16750184). This study has been partially supported by The 21st Century COE program 'Creation of Molecular Diversity and Development of Functionalities' at Tokyo Institute of Technology.

References

[1] Armand MB, Chabagno JM, Duclot MT. In: Vashishta P, Mundy JN, Shennoy GK, editors. Fast ion transport in solids. Amsterdam: North Holland; 1979. p. 131–6.
[2] Scrosati B, Schalkwijk W, editors. Advances in lithium-ion batteries. New York: Plenum; 2002.
[3] Gray FM, editor. Solid polymer electrolytes. New York: VCH; 1991.
[4] Bruce PG, editor. Solid state electrochemistry. Cambridge: Cambridge University Press; 1995.
[5] Wright PV. Br Polym J 1975;7:319.
[6] Ratner MA, Shriver DF. Chem Rev 1988;88:109.
[7] Tominaga Y, Izumi Y, Kwak GH, Asai S, Sumita M. Mater Lett 2002; 57:777.
[8] Tominaga Y, Izumi Y, Kwak GH, Asai S, Sumita M. Macromolecules 2003;36:8766.
[9] Kwak GH, Tominaga Y, Asai S, Sumita M. Electrochim Acta 2003; 48:1991.
[10] Kwak GH, Tominaga Y, Asai S, Sumita M. Electrochim Acta 2003; 48:4069.
[11] Cooper AI. J Mater Chem 2000;10:207.
[12] Sun YP, editor. Supercritical fluid technology in materials science and engineering. New York: Marcel Dekker; 2002.
[13] Condo PD, Paul DR. Macromolecules 1994;27:365.
[14] Handa YP, Zhang Z. Macromolecules 1997;30:8505.
[15] Kazarian SG, Vincent MF, Bright FV, Liotta CL, Eckert CA. J Am Chem Soc 1996;118:1729.
[16] Tominaga Y, Kwak GH, Hirahara S, Asai S, Sumita M. Polymer 2003;44:4769.
[17] Fontanella JJ, Wintersgill MC, Calame JP, Pursel FP, Figueroa DR. Solid State Ionics 1983;9/10:1139.
[18] Fontanella JJ, Wintersgill MC, Smith MK, Semancik J, Andeen CG. J Appl Phys 1986;60:2665.
[19] Bridges C, Chadwick AV. Solid State Ionics 1988;28–30:965.
[20] Fontanella JJ. J Chem Phys 1999;111:7103.
[21] Bendler JT, Fontanella JJ, Shlesinger MF, Wintersgill MC. Electrochim Acta 2001;46:1615.
[22] Armand M, Gorecki W, Andreani R. Proceedings of ISPE-2. London: Elsevier; 1990 p. 31.
[23] Lightfoot P, Mehta MA, Bruce PG. Science 1993;262:883.
[24] Reid RC, Prausnitz JM, Poling BE, editors. The properties of gases and liquids. 4th ed. New York: McGraw-Hill; 1987. p. 47.
[25] Lide DR, editor. Handbook of chemistry and physics. 81st ed. New York: CRC Press, p. 6–51.
[26] Abbott AP, Harper JC. J Chem Soc: Faraday Trans 1996;92:3895.
[27] Jun J, Fedkiw PS. J Electroanal Chem 2001;515:113.
[28] Dardin A, DeSimone JM, Samulski ET. J Phys Chem B 1998;102: 1775.